

OmniSoft: A Design Tool for Soft Objects by Example

Jeeeun Kim

jeeeun.kim@tamu.edu

HCIED Lab, Texas A&M University

Amanda Ghassaei

amandaghassaei@gmail.com

Creative Intelligence Lab, Adobe Research

Qingnan Zhou

qzhou@adobe.com

Creative Intelligence Lab, Adobe Research

Xiang ‘Anthony’ Chen

xiangchen@acm.org

UCLA HCI Research

ABSTRACT

Softness is one of the most important factors in human tactile perception. With recent advances in 3D printing, there has been significant progress in fabricating compliant objects. However, existing methods typically remain inaccessible to end-users, mainly due to the separation between designing shapes and setting printing parameters to achieve desired softness, resulting in the exclusion of its customization in early design processes. In this work, we contribute an end-to-end design tool that takes a design-by-example approach: given a 3D model, a user can specify the region of interest and a level of softness, by shopping everyday objects as a reference. The tool then generates both geometry and 3D printing parameters to reproduce the desired softness, which can be fabricated using low-cost FDM 3D printing and materials for it. We also provide a data-driven pipeline to enable other compliance modeling methods to be generalized within our design tool. In two user studies, we demonstrated that users could easily locate existing reference objects’ softness to a 3D printed object. In a design session, end-users successfully used OmniSoft to design augmented functions.

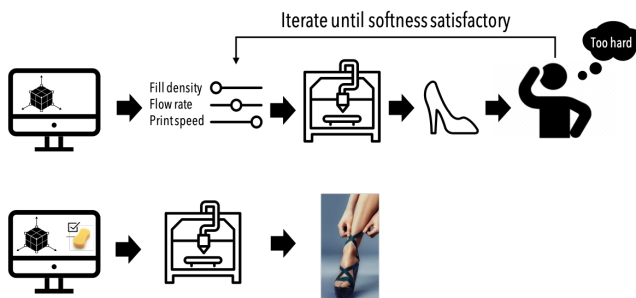


Figure 1: (top) The separation of shape design and slicer setting makes users tediously iterate fabrication, to achieve desired softness. **(bottom)** We propose OmniSoft, a design tool to regard softness as part of the *design parameter* using *familiar objects* to directly generate a ready-to-print file in G-code (Shoe photo by Graften.com).

Permission to make digital or hard copies of all or part of this work for personal or classroom use is granted without fee provided that copies are not made or distributed for profit or commercial advantage and that copies bear this notice and the full citation on the first page. Copyrights for components of this work owned by others than ACM must be honored. Abstracting with credit is permitted. To copy otherwise, or republish, to post on servers or to redistribute to lists, requires prior specific permission and/or a fee. Request permissions from permissions@acm.org.

TEI ’21, February 14–17, 2021, Salzburg, Austria

© 2021 Association for Computing Machinery.

ACM ISBN 978-1-4503-8213-7/21/02...\$15.00

<https://doi.org/10.1145/3430524.3440634>

CCS CONCEPTS

- Human-centered computing → Human computer interaction (HCI).

KEYWORDS

personal fabrication, softness, 3D printing, design by example

ACM Reference Format:

Jeeeun Kim, Qingnan Zhou, Amanda Ghassaei, and Xiang ‘Anthony’ Chen. 2021. OmniSoft: A Design Tool for Soft Objects by Example. In *Fifteenth International Conference on Tangible, Embedded, and Embodied Interaction (TEI ’21), February 14–17, 2021, Salzburg, Austria*. ACM, New York, NY, USA, 13 pages. <https://doi.org/10.1145/3430524.3440634>

1 INTRODUCTION

From bike handles to seat cushions to shoe soles, soft objects are essential parts of our daily lives. Recent advancements in 3D printing and increasing material options made it possible to 3D print objects with softness, showcasing the potential to expand the range of applications in low-cost 3D printers. However, designing and customizing the softness remain challenging for end-users due to the lack of a user-friendly language to express intention, the separation of shape design and parameter settings to interpret it in low-level machine language, as we call *communication gap*. Also, noting that each individual’s notion of *soft* depends on their prior knowledge and subjective experiences, it is hard to reliably offer perception-based design factors across many users. Thus, this gap limits users’ abilities to consider physical properties as in their design space. Existing design tools focused on shape and motion design, often through parametric interfaces. These tools do not make it better for designers to consider softness, as specifying properties has never been exposed to users at the early stage of design. Also, while it is technically possible to control softness by raw materials (e.g., TPU, Nylon) and through special micro-structures often referred to as metamaterials, these require tedious trial-and-error experiments in fine-tuning printing parameters (Figure 1 top) even for experienced users, as we call *execution gap*.

We present OmniSoft, an interactive design tool for end-users to specify desired softness by referencing everyday objects and create both geometry and printing parameters incorporated into Gcode (Figure 1 bottom). It bridges the *communication gap* between a user’s high-level language in describing desired softness and low-level machine language that 3D printers needs interpret it. As in industry where designers often refer to material swatches to directly feel the subtle differences between them, we take a similar approach to allow users to leverage prior experiences in perception and specify

subjective intents using those example. We conducted two user studies, demonstrating that human-perception well align with softness measured in standard scale and small softness difference is not likely to be perceptible. In the fabrication stage, we manipulate low-level printing parameters to achieve the specified softness computed from user's input, abstracting away machine-oriented details to close *execution gap*. To generalize the design approach for softness specification over many other existing metamaterial production techniques, we introduce a data-driven pipeline: (1) fabricating various samples and (2) measuring softness in a standard scale then (3) conducting a standard data fitting between factors in designing geometry and resulting softness, which can be referred and expressed by users' choice of reference example we propose.

OmniSoft addresses the following three challenges and limitations of other approaches:

Accessible While previous work has explored designing compliant objects (e.g., [29]), the lack of design support prevents many average users from applying these scientific findings. Often existing approaches require users to communicate their intent in special quantities such as Young's modulus [19], which is unfamiliar to users, assuming they know how to align microstructures that will produce global behaviors (bottom up, e.g., [11]). OmniSoft is top-down; users can regard softness in design time without barriers.

Affordable Many existing works often require high-end 3D printers or SLS for fine fabrication of micro-structures (e.g., [27, 31]). While recent works utilized FDM in part [19, 20], the complexity of the output design makes it time-intensive to generate geometry, slice, and print. In contrast, we exploit standard FDM printers and off-the-shelf materials to produce a fairly wide range of softness (2-95 in Shore A). Users also do not need to be equipped with a special input device to express haptic sensation.

Generalizable Although the modeling softness by simple slicing parameters is one benefit, our design process is compatible with other existing compliance modeling to 3D print soft objects. Using our data-driven pipeline, practitioners or researchers can fabricate a range of compliant samples using other materials and approaches, measure the samples' softness to quantify, then use standard data-fitting techniques to match their results to our library of reference objects.

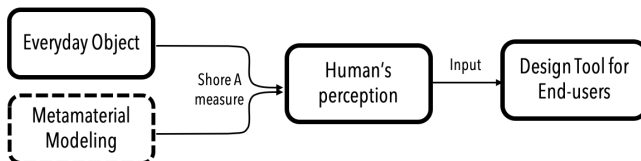


Figure 2: A data-driven framework can afford any compliance modeling methods to be used behind our general design tool to reproduce softness, expressed by everyday objects.

In a design session with 8 participants, we observed that even novice users can easily use OmniSoft, were inspired to design ample “functional” 3D objects using softness as a new design factor. OmniSoft abstracted away low-level expert knowledge from them, demonstrating it empowers end-users to consider softness as an

important design factor, proved by numerous novel application examples. Participants appreciated various aspects of design functions, suggesting future potential that are worth discussion in depth.

To summarize, we contribute with a insight of softness as a new design factor, a list of everyday objects with quantified softness for end-users to express design intent in the early stages of design, and computational interpretation of it into low-level printing parameters to afford low-fi fabrication method; bridging the gaps in both *communication* and *execution*.

2 RELATED WORK

We start by discussing recent works in metamaterial fabrication, modeling perception space for haptic sensation, and how this geometry-level information become accessible via interactive design tools.

2.1 Fabrication-Oriented Metamaterial Design

At a micro-scale, almost all material properties are the result of different structural arrangements at the molecular or crystal level, such as foams, bone porosity, and even gecko feet. Scientists have been intrigued by how such microscopic structures influence a material's overall properties for decades, by establishing theories of composites (e.g., [22, 23]), for example, how to obtain elastic behaviors by periodic microstructures [9, 33]). While these approaches were difficult to fabricate at the time, currently, manufacturing highly complex structures in millimeter and micron resolution becomes feasible with advancement of technology. In laser cutting [42] and computational weaving [35], researchers overcame the innate limitations of rigid materials, presenting controllable flexibility. In 3D printing, data-driven approaches have been used to design objects with desired deformation behavior [2]. More recently, different classes of periodically tiled cellular structures are combined to obtain desired global motions [27], mechanical functions [11] in both 2D sheet [32] and 3D shape [31]. In addition to regularly tiled patterns, a number of works explore the potential of using variations of Voronoi structures [18, 20]. Nonetheless, the structures used often require specific printing technology and printer settings even with the optimizational structure for FDM, such as continuity [19]. A small change in the printing parameters may result in completely different macroscopic material properties.

2.2 Perception-Aware Fabrication

Research in haptic interfaces, especially input devices, is increasingly concerned with user perception. In the context of digital fabrication, we can enable designers to consider the user's perception as a design parameter by identifying fabrication parameters that affect perception [28]. Awareness of such perception space allows researchers to understand what to consider when fabricating objects [29]. Findings enabled users to first 3D print two to three samples, perceive a discrepancy, then to choose a closer sample so the system can finalize the structural optimization with a user's choice. Yet, there has been little exploration of how to make this scientific finding available in user-friendly expression, and leverage it when designing 3D objects in regards to the expected interaction when fabricated. By abstracting quantifiable softness in a high-level language borrowed from familiar objects, our tool advances the

findings to be directly employed in the design time, not in the fabrication time. HapticPrint offers the capability of designing external (surface textures) and internal (weight and resisting force) tactility [39]. Medley further provides a list of embeddable materials and a design tool to support post-processing 3D printed objects with mechanical functions [3]. Human perception of compliance has been a hybrid topic that spans multiple research fields that include localizing true stiffness through perceptual space in psychology [8, 37] and psychophysics [10, 12], generating such sensation for interaction [17] and identifying various cues affecting this sensation [38] in haptics, measuring sensation using neuroscientific approach [6, 30], producing programmable compliance by geometry optimization in mechanics [22] and computational fabrication [28, 29], and more. Instead of competing with one or more previous works, our goal is to leverage findings from these works in developing an accessible, example-based design process, enabling users to leverage prior experiences with everyday objects.

2.3 Design Tools for Interactive Fabrication

Interactive tools are useful for end-users to explore a design space, especially in the early stages of design [4]. With a goal of enabling rapid prototyping, speeding up iteration became a first-class challenge, leading to approaches that allow users to quickly validate results (e.g., [25]). Instant visual feedback takes a significant role in this case, allowing users to estimate shapes based on suggested variations (e.g., [5, 13]), and predict mechanical behaviors (e.g., [21]). In the web design domain, an example-based design has been already on the rise to support reproducing target content [14] through browsing and borrowing concepts from galleries [16] and then variate for the improvements. Yet, these tools focus on *visual* features, namely shape and motion behavior. Designing non-visual properties (e.g., softness) still remains a challenge for casual users.

To summarize, recent work has expanded the capacity of digital fabrication tools to manufacture not only shape, but the functional properties of objects, such as compliance. However, few tools expose these advances in a way that it is accessible to end-users, which hinders the wide adoption of these techniques by wide audiences.

3 DESIGN WALKTHROUGH

Here we introduce a step-by-step walkthrough of OmniSoft design process. We suppose Cathy, who wants to design a bike seat (a hypothetical user inspired by one of our participant's designs).

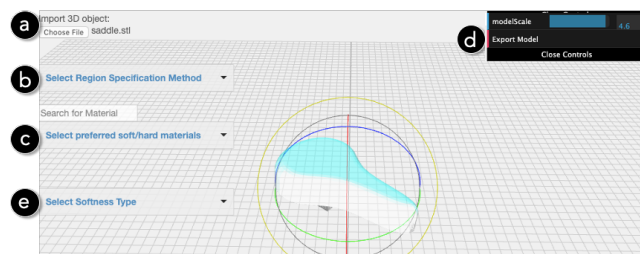


Figure 3: Menus progressively appear with sub design tasks, to show a step-by-step design process.

Step 1. Importing a 3D Target Object Cathy is designing a new bike saddle because her hand-me-down bike hurts when riding. She found a model online, downloads it, and imports into OmniSoft. OmniSoft shows design actions in sequence from left-top to bottom to progressively guide a user through the design process, import a model (Figure 3a), specify the region to be soft when printed (Figure 3b), then shop examples to specify the desired softness(Figure 3c). Sub-tasks also subsequently appear upon the user's choice, such as choosing the type of interaction, detailed in the following sections.

Step 2. Selecting Expected Interaction Type and Region of Interest Cathy then selects “*by the interaction type*” to specify the region, which will take place when the saddle is printed. Then OmniSoft shows a supplementary list of interaction types: press by a finger, step on by a foot, sit on by hips, grasp by a fist, or squeeze by two fingers (Figure 4).

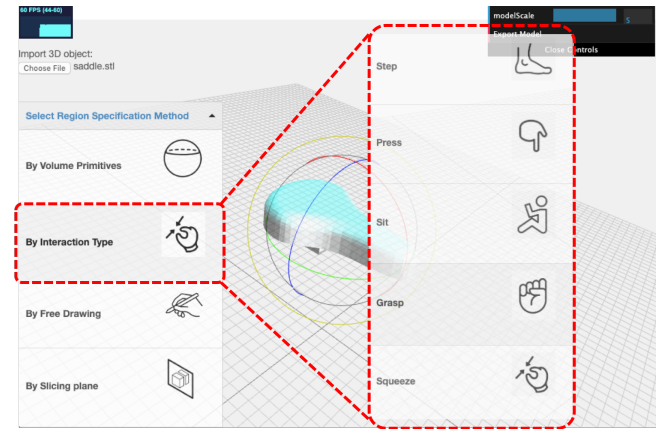


Figure 4: Five body parts that interface with a resulting object are listed as options under ‘interaction type’

Selecting “*Sit*” retrieves a 3D mannequin with sitting pose, to show body parts that will interface with the target 3D object when fabricated. Cathy can see the effective region by a shadow projected onto the surface, with an arrow indicating the direction in which the force will be applied (Figure 5). Thus, she can estimate (and later re-scale) the dimensions relative to the body, which is pre-scaled according to average adult sizes. She can also scale the body if she is designing one for her son. Future work could additionally provide an interface for users to input their own hand or foot size and automatically scale projected body parts.

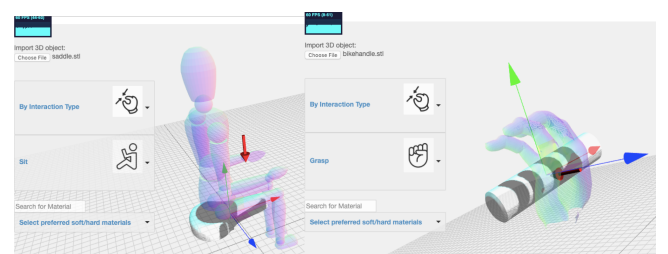


Figure 5: A user drops shadows of the interfacing body to specify region, for example, sitting and grasping.

For other cases, OmniSoft also provides four options to select the desired soft region. For example, when designing a high-heel, a user can: (1) specify the type of interaction with which the resulting object will be used (Figure 6a), (2) split the model by a cutting plane (Figure 6b), (3) perform a boolean intersection using a solid 3D volume (e.g., sphere, cube, cylinder, and torus, as shown in Figure 6c), or (4) sketch a free-form drawing of a region on the surface (e.g. Figure 6d).

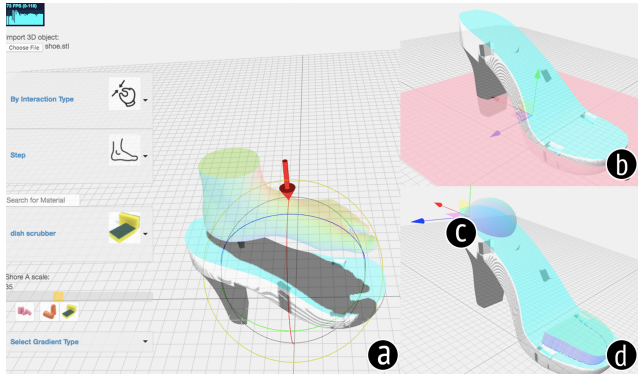


Figure 6: Four methods to select region of interest from global shape: by (a) interaction, (b) slicing, (c) 3D volume, and (d) drawing

Step 3. Specifying Desired Softness by Examples Next, Cathy specifies the softness level by browsing a list everyday objects, which are listed in ascending order from soft to hard, or searching by keyword (Figure 7). She first chooses a makeup sponge but cannot remember how soft it is, so chooses earplug and can-cooler as she thinks they are similar. For anyone not familiar with any given materials from the options, we provide many other similarly-soft objects nearby; OmniSoft shows relative softness in a slider bar to let users explore the ranges in between (Figure 7 left). OmniSoft visualizes changes applied to the target 3D object in real-time, as Cathy explores the range.

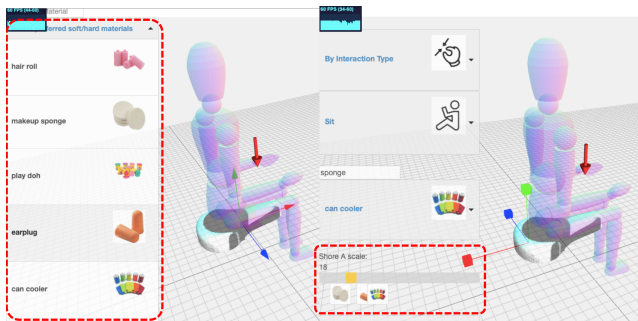


Figure 7: A user can choose a reference to specify desired softness (left), or multiple materials to adjust the level in a given range (right)

Step 4. Exporting a Ready-to-Print File When the design is finished, a new geometry is generated incorporating an internal

structure to reproduce the intended softness in her target region of interest (Figure 8). Clicking the “Export” button generates a ready-to-print file. OmniSoft exports a result in standard G-code, that can be directly fed into any commodity 3D printer, without needs to consider complicate settings of low-level parameters. Finally, Cathy can mount a new bike saddle printed in one material with a comfort seat and rigid body to safely install the parts onto her bike.

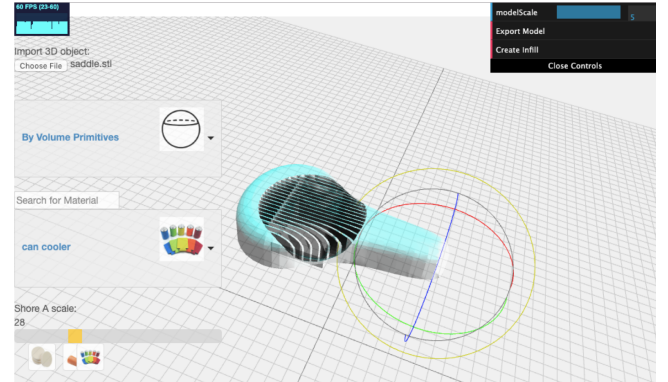


Figure 8: A user can see and validate the density of structure as she adjusts softness for generating a ready-to-print G-code file

4 RESEARCH QUESTIONS

Our objectives of (1) enabling users to specify softness using familiar objects and (2) implementing the system to reproduce intended softness using low-level printing parameters were motivated by the following two questions:

RQ1: How can 3D printed softness be controlled by low-cost FDM slicing parameters?

RQ2: How can users associate desired softness to these low-level machine languages, to utilize softness as design factor?

5 COMPUTATIONAL PREDICTION OF SOFTNESS BY SLICING PARAMETERS

We first modeled softness using printing parameters and evaluated if reproduced softness matches users’ perception. In this work, we define *softness* in the same manner as the seminal work [36], where softness measures a material’s deformability under force. Specifically, we employ a standard softness measuring principle using the Shore A hardness scale [15], which measures the resisting force against indentation, a predefined displacement.

5.1 Gaps in User & Machine Language

Taking into account the fact that low-level printing parameters are the factors that affect printed objects’ softness, we noticed a gap between these low-level machine language and user’s high-level design expression. We first investigated the correlation between printing parameters and the measured softness of printed objects. Shore A scales can be easily measured with a Durometer¹. This

¹Details available at https://en.wikipedia.org/wiki/Shore_durometer

handheld device is portable, cheap, and easy to operate by non-experts, thus are commonly used in the plastics industry to measure a wide range of products such as rubbers, vinyls, etc. Another benefit of using the Shore A is its potential to convert it to *Young's modulus* which has been used in many prior works, with reasonable accuracy and range between 30A (corresponding to a laptop protector insert foam) and 95A (a garden hose) [15]; this makes our approach compatible with other metamaterial production methods, if they utilize Young's modulus in measured compliance.

5.2 Slicing Parameters that Affect Softness

Printing parameters are so far used to calibrate and fine tune the quality of 3D prints. These parameters are typically set in slicing programs such as Cura and Slic3r, compile a 3D design file (user-friendly) to a command file (machine-friendly). A list of parameter values set for specific settings generate a physical model with different material properties, such as strength and density. Within Cura, a popular open source slicing program, the expert settings expose advanced parameters that affect quality and other properties in printed artifacts. To find the most significant factor that affects softness, we set three criteria:

- **Printability (P):** changes in the parameter should ensure that low-cost FDM machines print fine-quality object with low chance of failure.
- **Range of softness (R):** changes in the parameter should generate a wide range of softness.
- **Granularity (G):** changes in the parameter should be able to fine-tune softness.

To evaluate the effect of parameters on produced softness, we sampled each parameter around its default value, and printed 10-15 cuboids in $30\text{mm} \times 20\text{mm} \times 10\text{mm}$ its size in varying conditions, as shown in Figure 9.



Figure 9: Example samples printed in softness of 30.5, 40, 42, 45.5, 73.5. Other external factors (size, color, and exterior textures) are identical.

As we printed samples within *printable (P) range*, so once the print fail occurs due to extreme condition, we set those condition as min/max bound. For example, in $>0.25\text{mm}$ layer height, external wall layers detach each other, and we cannot decrease print temperature below 180 degrees. For each sample, we measured softness at three different locations on the top surface over two iterations, with a cap that can reduce effects of porous materials by the needle. We printed in off-the-shelf flexible filaments (e.g., eSUN Soft PLA and NinjaFlex TPU) to guarantee accessibility. While objects printed using these materials are very stiff if printed in the full density of 100% (softness ranged 85-95A, following the original property known by the manufacturer), processing in cautiously selected parameters can generate fairly *squishy* objects as demonstrated in

	Printability	Range	Granularity
Layer height			○
Shell thickness	○		
Flow rate			○
Print speed			○
Top cover count	○	○	
Infill type	○		
Infill Density	○	○	○

Table 1: Printing parameters with varying effects. Only infill density meets all three criteria.

existing works (e.g., [7]). Experimental conditions are detailed in Appendix A, Table 3 with summaries on empirical findings.

From findings, we can conclude that infill density is the most promising variable for programmable control of softness that meets our three criteria; it reproduces a wide range of softness (R), with fine tunable softness (G), and guaranteed print quality (P), as summarized in Table 1. Although this paper centers the premium at the simplicity, others present potentials to fine tune softness given other slicing parameters such as geometric constraints, that we will discuss more in detail in the discussion.

5.3 A Data-Driven Pipeline to Model Softness

Infill density is defined by the percentage of internal solid volume per the entire volume of an object. Denser infills leave less empty space inside the object; infill density is determined both by the number of interior structures (e.g., # of walls), and the thickness of these structural walls. Often, the wall thickness of the infill is tied to the nozzle diameter, which cannot be altered without hacking. To simplify our experiment about *density*, we controlled it by adjusting the gap [40] between the parallel blade walls, as this approach allows us exclude other confounding factors, such as extra binding strength with a top cover in cross sections in grids. For example, the count of cross sections in the same density could be different as shown in Figure 10 due to the placement of the object on the print-bed, which affects resulting softness.

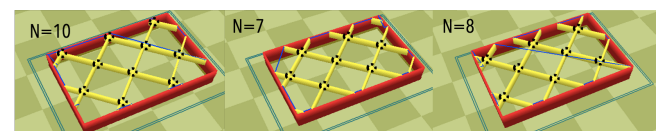


Figure 10: Different numbers of cross-sections (highlighted in dotted circles) with the same density (10%) can confound measured softness

For fine-evaluation of infill density, we 3D modeled 15 cuboid samples within the same dimensions ($30\text{mm} \times 20\text{mm} \times 10\text{mm}$) and varying interior wall spacing that are in 0.4mm thickness, and printed using a MonoPrice Maker MK11 with a 0.4mm nozzle. We kept all other printing settings constant but iterated twice with two commonly used flexible materials for FDM, SoftPLA(eSUN) and TPU. We measured the softness of each sample under a vertical, downward force. Then we conducted standard data fitting to get a

model that adequately predicts a wall spacing computed from input softness, where spacing (L_d) is computed as:

$$L_d = e^{-1/\beta \times (\ln S - \ln \alpha)} \quad (1)$$

S denotes target softness with $\alpha=43.9$, $\beta=0.415$. For the details of the data fitting process, see the Appendix B.

Replicability: Other Machines

Validating whether our approach is replicable using other types of machines, we further iterated experiments using three commodity FDM 3D printers: MonoPrice and Printrbot with 0.4mm, as well as Lulzbot with 0.4mm and 0.5mm nozzles. Samples were printed in the same profiles (layer height 0.2mm, shell thickness 0.25mm, bottom/top thickness 0.4mm, print speed 20mm/sec, temperature 220C, flow rate 110%) and presented similar softness (difference is STD=0.94A, less than 1A); in either print in heated (Lulzbot, MonoPrice) or not-heated (PrintrBot, MonoPrice) bed.

Generalizability: Other (meta)materials

We further validated our prediction model with other types of flexible materials, in addition to TPU, the most widely used flexible material. We iterated the experiment on new materials (Soft PLA and PolyMaker PolyFlex, 90% TPU + 10% PLA). Figure 11 shows the relationship between measured softness and wall spacing for all three materials. The data follows similar trends, and the slope follows material's natural Shore A; samples printed with a material of 95A are relatively stiffer (higher softness values in the same data points) than samples printed using filament with 85A.

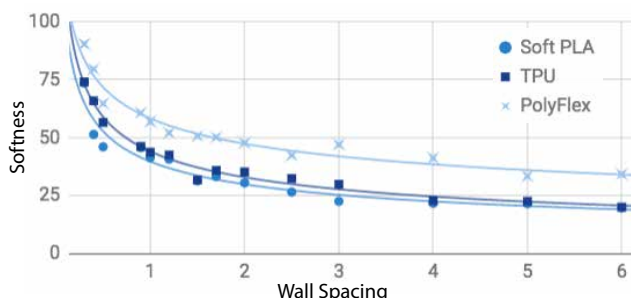


Figure 11: Two materials with the same Shore A (SoftPLA and TPU, 85A) exhibit nearly identical wall spacing to softness correlations. A material with a higher Shore A rating (PolyFlex, 91-5A) shows a similar trend, but is stiffer overall ($R^2 = 0.95, 0.98, 0.95$, respectively.)

In summary, material experts and practitioners can iterate our approach by: (1) printing a number of samples with varying softness modeled by unique geometric/material features, (2) measuring generated softness in Shore A, (3) operating a standard data fitting to find the correlation with the variables that affect softness to find new constants in our prediction model. In the case for using the same geometric structure but only varying raw material, or simply to calibrate in different machine type, practitioners can use our open sourced process with provides samples in STL and suggested settings to ensure printability. The system then finds a new coefficient and intersect (α, β) to redefine correlation between input

softness and computed wall distance. Either case, our front-end design tool remains universal, as end-users still can specify desired softness using the same expression—familiar objects to inform S value for computation.

6 PRIOR EXPERIENCE AS REFERENCE

Expanding known everyday objects for Durometer [34] measure, we collected more examples that are familiar to us. Then we measured the Shore A using a commercial Durometer, which makes it possible for *anyone* to utilize it to add more objects to the list to expand the library shown in Figure 12. Although we only included objects in softness range 2-95A that are reproducible using FDM, it covers almost full range that commercial Durometer can measure. Note that we do *not* exclude objects with nearly the same softness. Therefore, for example, a user who knows the feeling of a flip-flop ($S = 40$) but is not aware of how soft a bottle nipple ($S = 40$) is can still choose one more familiar.

Reference Object	S	Reference Object	S	Reference Object	S
Hair roller	2	Drawing eraser	25	Wiper blade	60
Make-up sponge	2	Laptop-safe Insert	30	Silicon watch bands	70
Ear plug	7	Vinyl toys	35	Shoe heels	70
Cooling sleeve	9	Flip flop platform	40	Pencil eraser	73
Gummy jelly	10	Bottle nipple	40	Skateboard wheels	78
Mouse pads	16	Bath toys	42	Leather belt	80
Rubber bands	17	Door sealer	55	Shoe sole	80
Dish scrubber	21	Car tire	60	Garden hose	95

Figure 12: Example objects we found and their softness we measured to be used as input (in Shore A).

7 QUANTIFYING PERCEIVED SOFTNESS

Partly due to inaccurate human perception, we do not need to “exactly” reproduce target softness; we only need to emulate relatively similar softness. The key hypothesis here is that users perceive softness in a way that roughly corresponds to how it is described by the standard scale (e.g., a lower number on the scale indicates a softer material), so they can quantify desired softness by referencing similarly soft everyday objects.

Here we introduce two studies to validate this; The first study shows that users are able to order softer objects to harder objects as ranked by the standard scale. The second study demonstrates that a reference object can almost accurately represent the sample printed to reproduce the same softness. We do not let users point to the specific value, as it is not realistic that users can appreciate what those values mean.

7.1 Study 1: Measured vs. Perceived Softness

Here we evaluate whether the softness measured by the scale match the softness felt by a user (Relative).

7.1.1 Method and Apparatus. We recruited 20 participants (Male=12, Female=8, age=21-32). We first ranked the 3D printed cuboid samples (shown in Figure 9) by the Shore A scale, from the softest to the hardest (1-14). The softness adjacency between two samples varies (diff ranging from 0.1 to 22). We let users order samples from the softest to hardest, then compared these subjective rankings with the true ranking implied by the standard scale. We directed users to poke on samples using one finger at a time, with a vertical motion to avoid anisotropy. However, we did not control the finger velocity when pressing which may affect human perception [6], as it is more realistic to measure humans' interaction. If tested with the same speed or force, it would better to be tested using a machine as in [39]. Structures were printed under the thin one top cover that encloses internal structures, with the same color (white) and size to prevent any additional visual cues.

7.1.2 Results. Figure 13 shows a confusion matrix relating the actual softness ranking (measured in Shore A scale) and users' perceived rank. Participants' relative softness ranking mostly follows the true ranking. Discrepancies in a particular instance is off at most one or two rank. The diagonal trend in the matrix indicates that users' perception is similar to the true ranking in standard softness. As we hypothesized, small differences (e.g. sample 2 & 3 with only a 0.1A softness diff) are barely perceptible to users, whereas two objects with obvious differences (e.g. sample 13 & 14 with a 22A softness diff) are easier to order with no confusion. This implies that even when the softness modeling cannot exactly reproduce the level of softness (e.g., diff in input and output softness STD: 0.94, shown in Table 4 in the Appendix B), their differences would generally not be noticeable to users as it is under *just-noticeable difference*. We conclude that (1) humans will perceive a level of softness that approximately follows as described in the standard scale and (2) small differences in softness are not perceptible.

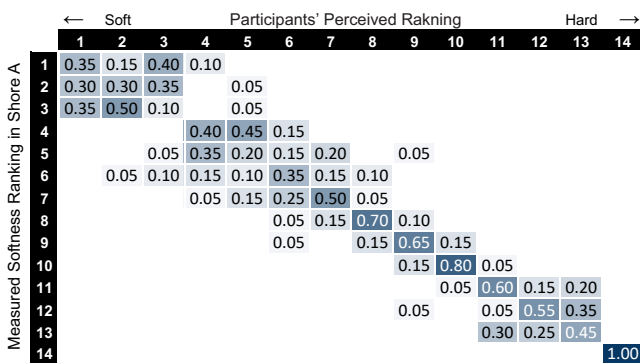


Figure 13: Users perceived confusion over true softness ranking. White cells indicate no confusion observed.

7.2 Study 2: Finding Matching Opponent

Although our model can reproduce the softness that matches the user input, users' expression uses their own subjective sense. The next challenge is how to enable individual users to describe their desired level of softness, not by parametric values; What can "softness 9" mean to end-users, and how will this be perceived by individuals with different sensitivity? There are existing methods to simulate the physical softness using a special device [24, 26], allowing users to give instant feedback on whether a presented softness is satisfactory. However, the special devices are often expensive and not always available, thus, most users cannot access to such supplementary devices. Instead, users can retrieve the desired softness by leveraging their *previous sensory experiences*.

7.2.1 Method and Apparatus. The second study tests whether a reference object could accurately represent fabricable-softness. We recruited 29 participants (Male=18, Female=11, ages=20-49), not overlapping with the first study. We provided three existing objects with varying softness, ranging from a very soft dish sponge ($S = 21$), to a flip-flop in medium softness ($S = 40$), to a very hard pencil eraser ($S = 73$). None of these were manipulated after purchasing them from stores. Providing 3D printed samples with varying softness in a random order (the same set of 14 samples used in the study 1), we asked participants to compare the softness between the given everyday objects and printed samples, then to find the match amongst 14 sample objects (e.g., find one sample that has the same softness of a flip-flop). Participants conducted their search without any predefined ordering of the three reference objects; however, as their finger may feel tired as the study proceeded, we encouraged them to take breaks after arriving at a match for one instance before moving on to the next.

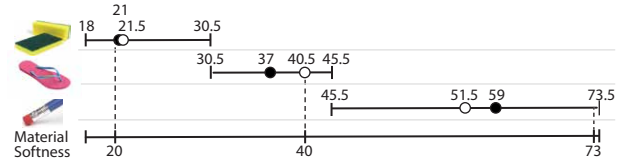


Figure 14: Perceived softness range of existing objects. Each range shows the minimum and maximum values of softness paired. The black dot indicates the mean, and the white dot indicates the median of participants' choices. The observed median softness is very close to the actual softness of the first two objects. Due to the sparsity of the provided softness, the perceived softness for the third object is noisier.

7.2.2 Results. Figure 14 summarizes the comparison between the softness of the given everyday objects (that will be used as reference to specify desired softness) and the cuboid samples in varying softness. Most participants were able to find the matched counterpart of a reference object (with average errors of 2.5A for the flip-flop, 4.1A for the dish scrubber, and 18A for the pencil eraser). Many of the participants ($N=15$) had difficulty in matching the pencil eraser ($S = 73$) between the hardest sample (softness 73.5A) and the second hardest sample (51.5A), mentioning that the eraser's softness felt somewhere between the two, which is even the more

accurate comparison. If we provided a closer sample softness, we can imagine users should be able to locate it. We conclude that humans can match the softness of a reference object with reproduced sample of similar softness.

From both studies, we reconfirm that users perceive softness in a way that roughly corresponds to a standard scale, so they can cite desired softness by referencing an object with quantified scale that are similar to the target.

8 IMPLEMENTATION

Integrating empirical findings found above, we implemented OmniSoft interactive design tool for end-users. The design tool was developed in Javascript with supplementary libraries including THREE.js and CSG.js for mesh manipulation and graphics operations. The tool is offered as a web-application, accessible by anyone with a modern web browser. We open sourced our design tool on Github², thus, advanced users may add more reference examples with their Shore A values and other design parameters, such as specific brand's sole softness.

For region specification, 3D shape primitives (e.g., sphere, torus, cube, etc.) are overlaid by its center hovers over the target object's surface; in this way, a user can easily specify the contact region, ensuring the soft region is not completely obstructed by surrounding rigid parts. Similarly, free-form sketches are carried out by a pen hovering along the object's surface. Drawing automatically creates a closed loop, then projected onto the XY-plane and linearly extruded to create a volume. Now a 3D shape is overlaid with the target 3D object to allow scaling or re-positioning, if needed. Later, shapes are intersect from the source 3D model and filled with internal walls. Given the bounding box size of the shape and the user-selected soft object, wall spacing is determined to build parallel 0.4mm blade walls (See Appendix B for the computation detail and validating the prediction results), placed in the region of interests. Remaining regions remain rigid by filling in 100% infill to keep the global shape when external force is applied (e.g., high-heel). Finally, the system runs the CuraEngine[41] back-end, to export a ready-to-print gcode file directly, which sets all other printing parameters to the best profile to produce a desired softness. Currently the tool sets machine-specific start Gcode optimized for Ender3, while enabling users to select machine types using a drop-down GUI is a future addition, so the information can be passed as command arguments that CuraEngine supports.

9 DESIGN SESSION

We observed usecases of OmniSoft to see (1) if users can create soft objects without any barrier and (2) if providing softness as design parameter sparks creative ideas.

9.1 Participants, Task, and Procedure

We recruited 8 participants (male=5, female=3) with various backgrounds, including social science, engineering, and industrial design. Table 2 summarized their demographics and design choices. First, we showed several cuboid samples with varying softness and informed that the samples were 3D printed using one material,

only adjusting printing parameters. Then we walked through the design tool using a high-heel example (10 min). Next, we asked participants to brainstorm their own ideas, encouraging to search 3D models online. The screen was recorded by Quicktime player to log participants' workflows. We conducted a semi-structured interview to identify challenges and opportunities they revealed.

Exp*	Design Object	Region	Chosen reference
P1	0	Bike saddle	Interaction >Flip-flop
P2	0	iPad stand	Drawing Laptop protector
P3	1	Chair & Handle	Volume Eraser
P4	2	Stool	Plane Dish scrubber
P5	0	Headboard	Interaction Flip-flop
P6	0	Helmet	Volume >Gummy jelly
P7	0	Guitar	Drawing Dish scrubber
P8	0	Table & Spatula	Volume <Rubber band

Table 2: Participants' 3D object designs with region and material specification for softness. (<> indicates adjusted softness using a slider, *Experience level, 0: no experience, 1: causal experience, 2: expert)

9.2 Results and Findings

Six participants were able to finish task in less than 30 minutes. Most created a single application, but two participants (P3, P8) generated two, while the others verbally explained more ideas. Due to the current size limitation in the desktop 3D printers, we were not able to print all results at full scale (e.g., furniture, guitar) but we printed selected examples as partly shown in Figure 15.

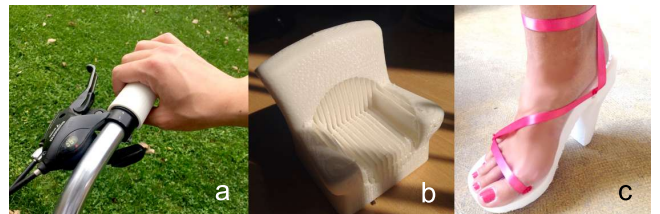


Figure 15: A printed bike handle in custom-grip, a furniture (in toy size) and a high-heel with personal comfort.

Overall, all participants successfully utilized softness as design parameter, being inspired to create a wide variety of products as showcased in Figure 16.

Outcomes demonstrate that OmniSoft generates new expressive possibilities. All appreciated the new way of thinking 3D design beyond shapes, a simple pipeline and straightforward way of specifying softness. They appreciated different aspects of the tool, which presented us ample areas to discuss more in depth.

Softness as a Factor to Specify Function An industrial designer (P4) enjoyed redefining the stool from his own furniture design portfolio, with a soft cushion on top. Inspired by the opportunity the tool grants, P7, a material engineer, designed a *custom comfort* guitar which will not hurt his thigh when playing; he drew a region where he feels ache (Figure 16e). Finishing the design, he noted “*I have struggled explaining the quantitative definition to*

²<https://github.com/qubick/OmniSoft>

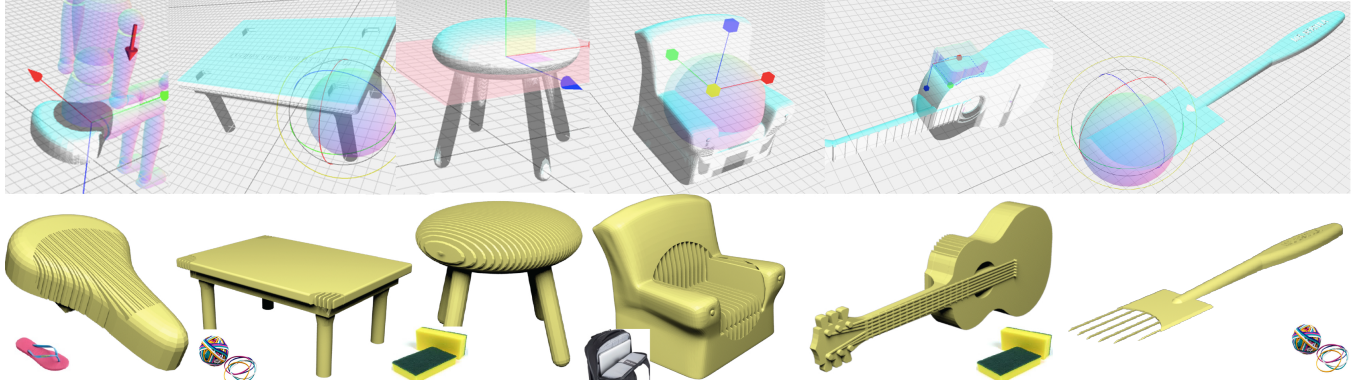


Figure 16: Designs created by our study participants: an ergonomic bike saddle, child-safe table, stool and sofa with an embedded cushion, a comfort guitar, and a soft cooking spatula. We created openings on the surface to reveal internal structures to produce softness. Insets represent users' choice of reference objects.

describe obtainable function. [...] the idea of using what people have experienced already is so intuitive, I will adapt these references to explain my own research as well". P8 created a set of furniture with baby-proof corners (Figure 16b), while leaving other parts rigid to keep their original function. P8 also created a 3D printable spatula to stir a cooker without scratches. Diverse product ideas provided us insights that users consider softness as opportunities to *specify functions*, beyond the shape design. Some users liked the idea of selecting parts to be printed with such functions using just one material, than the ability to relate their desired softness. For example, P3 mentioned that "This (baby-proof furniture) is just to make it safe, I wouldn't be bothered even if the resulting stiffness is slightly off." P2 added "Subtle softness difference doesn't really matter to me as we people are not that precise to notice that", similar to findings from our study 1.

Structural Effects Created by External Geometry It is possible that the region near the rigid wall feels harder than the center. Yet, participants did not expect the specified region to present uniform softness. They supposed regions near the other rigid parts would gradually become stiff, feeling that they created *structure*. For example, owing to this natural gradation in softness distribution, P3 thought that he created a handle with a *grip position* instead of uniformly soft cover and exclaimed: "A steering wheel to inform novice drivers the standard grip position would be a cool example." For users who may want more evenly applied softness, we consider optimization by gradually decreasing infill density or decreasing flow rate to lower the softness, in relation to the distance from the center as future work. As part of this, we left choice of the region segmentation type (i) binary or (ii) gradation (Figure 3e) to users, so they can make the decision. As we created the internal walls uniformly (10mm high, the dimension of the cuboid samples) from the contact surface, there was no discrepancy by the scale of the object in the softness created and perceived.

Potential Softness Discrepancy by Interaction Mode From many new applications we saw from the design session, we noticed that users' perceived softness could vary upon the actual interaction mode; what if the user specified the softness remembered from *squeezing a sponge* to design a shoe, which will be *stepped on* by

a foot when 3D printed? Due to current limitation of in-person studies, we provided actual prints only to selected participants and asked if there were any discrepancies. "I imagined the softness reminding of the interaction I had with that object (flip-flop). I adjusted the value using a slider, as I thought that it could feel softer if I sit." (P1) "As long as generated softness is the same when felt using the same interaction I used for measuring, I am happy with that." (P3) We believe size limitations of FDM printers will soon disappear, allowing us to fabricate models in various scales to test haptic sensations felt by different body parts in actual interaction (sitting vs. squeezing). Evaluating users' perceptual space in depth to see if the produced softness matched their expected interaction modes is an interesting future direction, where visualizing deformation could be part of this work.

Advanced Interaction Mode We also identified several remaining challenges in the tool, specifically regarding interaction modes. We currently do not support specifying dynamic interactions; for example, in designing the softness of a bike seat, P1 wanted to animate the mannequin's legs as if s/he was riding a bike. Also, some contacts were unexpected by our tool, for example, P5, who failed to specify a region in the first trial, wanted the mannequin to *lean* on a bed headboard. The region is defined by the light cast from the top light of the scene; instead, the facilitator helped rotate the headboard in the X-axis, so the back of mannequin can be used to specify region by the shadow without a "leaning" interaction supported, which is worth it for future tool design.

10 LIMITATION & FUTURE WORK

Our approach requires the use of innately soft material (TPU, Soft PLA, Nylon, etc.,) to achieve wide range of softness over relatively flat surface, and is not applicable to rigid plastic (e.g., PLA/ABS). Otherwise, subtle differences by adjusting slicing parameters would not be perceptible. Beyond this, we discuss the potential to expand our work in various directions.

10.1 Exploring Other Printing Parameters

As described earlier, we centered on the effects of *density* of inner space. We focused on parallel walls so to control other additional

confounding factors such as different number of cross-sections. However, different infill patterns define overall density (often presented as percent in slicing software) by different criteria, and may also vary their Young's moduli [19]. Connections between infill walls, such as in honeycomb or grid patterns, may strongly bind with the exterior shell. For the future, we need to consider the correlation between the slicing area and the number of cross sections appearing as well as the empty space which needs deeper understanding in slicing algorithm. Note that such patterns with more cross-sections are not recommended for flexible material printing, as higher viscosity in the glass state results in many gaps and holes appearing on the top cover in practice. Additionally, the bending and buckling behavior of the infill dramatically changes according to its geometry, as also observed in our preliminary experiments. One direct future work would be to repeat our printer parameter testing on additional infill patterns and same pattern under various external geometry (e.g., complex convex) and report how these affect controlling softness. Although not all printing parameters tested in our experiments met the three criteria (Printability, Range, Granularity), they can contribute to fine-tuning. For example, higher flow-rate can harden the softness within the same line distances, while printing in higher temperature increases porosity of a prints which makes it softer. Albeit there exists limited range these can be applied, utilizing various print parameters fills the gap that is otherwise not achievable only by density.

10.2 Other Mechanical Characteristics with External Geometry

Expanding the above experiment, we would like to simulate and visualize additional mechanical behaviors of these internal structures. Prior work investigates non-uniform softness over the regions that are under different external shapes [29, 31]. Currently, we are concerned with one density type across a selected region; our future goal is to allow users to control other mechanical properties in one region, such as spatially varying softness, weight, and buoyancy. In our tool, users can specify multiple regions but only one softness level per region. To simplify the experiment, our methods only tested user interactions along the surface normal, but it is possible to control the direction-dependant mechanical characteristics of 3D printed objects, such as orthotropic or anisotropic resistance around a surface contact [32] that may change a user's landscape for interaction design with a 3D printed object.

10.3 Printing Structures along Non-Axis-Aligned Directions

FDM printing innately presents limitations on printing directions. Our approach to build infill is based upon vertical structures supporting a perpendicular contact surface. When designing anisotropic responses, it could be essential to build infill patterns that are not orthogonal to the printing direction as they also present unique properties on the surface [1, 20]; this also applies to organic shapes whose contact surface and infill does not intersect orthogonally (e.g., spherical surface [29]). In future work, we will investigate generating these infills and optimizing printing direction to guarantee printability.

10.4 Softness Perception by the Mode of Interaction with Objects

Humans' perceived softness of objects is also dependent on the interaction methods. For example, as also reported as findings from the design session, an object's perceived softness level may vary if a user pokes it with a finger versus presses it with an elbow, partly due to the distributed force on the surface [1], the amount of force applied, and velocity of these interactions [6, 8]. Similar to the prior work, we assumed no velocity dependencies on resulting perception [29]. Further in-depth user studies should evaluate how users perceive the same softness differently based on their mode of interaction. In the future study, we will print samples with a varying softness and ask users to rate softness based on various interaction conditions, including (1) poking, (2) squeezing, (3) stepping, and (4) sitting, potentially considering the (average) velocity in varying interactions. We will measure the differences in perceived softness to quantify and develop a new model that reflects changes. This relation can be used in automatic adjustment upon users' selection of softness reference, in reproducing resulting softness by *expected interaction* type as input. Existing work of letting users specify direction and amount of force expected to be applied to an object [5] could help reflect user needs in softness adjustment.

11 CONCLUSION

Despite recent advances towards democratizing fabrication, the first-order effort has been made to improve the efficiency and precision of existing practices by expediting iteration. Only a handful of sufficiently accessible user interfaces exist that incorporate human perception as a design factor and allow end users to utilize them in the early design stage. The design has been detached from production, resulting in missed opportunities for end-users of expanding their design space with machine parameters that affect product properties. With OmniSoft, users are able to design and fabricate soft objects using a high-level expression borrowing everyday examples. Through an intuitive interface that abstracts away low lever expert knowledge, users can convey design intent in the early stage of design, to affordably produce desired softness by a low-fi fabrication method.

ACKNOWLEDGMENTS

Authors thank Doyoung Park and Clement Zheng for discussion during the early stage of this work, Wilmot Li for his expert feedback, and Cuong Nguyen for his advice to improve the presentation. This work has been partly supported by Adobe PhD Fellowship and Adobe Gift Award.

REFERENCES

- [1] G. Ambrosi, A. Bicchi, D. De Rossi, and E. P. Scilingo. 1999. The role of contact area spread rate in haptic discrimination of softness. In *Proceedings 1999 IEEE International Conference on Robotics and Automation (Cat. No.99CH36288C)*, Vol. 1. 305–310 vol.1. <https://doi.org/10.1109/ROBOT.1999.769996>
- [2] Bernd Bickel, Moritz Bächer, Miguel A. Otaduy, Hyunho Richard Lee, Hanspeter Pfister, Markus Gross, and Wojciech Matusik. 2010. Design and Fabrication of Materials with Desired Deformation Behavior. *ACM Trans. on Graphics (Proc. SIGGRAPH)* 29, 3 (2010).
- [3] Xiang ‘Anthony’ Chen, Stelian Coros, and Scott E. Hudson. 2018. Medley: A Library of Embeddables to Explore Rich Material Properties for 3D Printed Objects. In *Proceedings of the 2018 CHI Conference on Human Factors in Computing Systems* (Montreal QC, Canada) (*CHI ’18*). Association for Computing Machinery,

- New York, NY, USA, Article 162, 12 pages. <https://doi.org/10.1145/3173574.3173736>
- [4] Xiang 'Anthony' Chen, Jeeeon Kim, Jennifer Mankoff, Tovi Grossman, Stelian Coros, and Scott E. Hudson. 2016. Reprise: A Design Tool for Specifying, Generating, and Customizing 3D Printable Adaptations on Everyday Objects. In *Proceedings of the 29th Annual Symposium on User Interface Software and Technology* (Tokyo, Japan) (*UIST '16*). ACM, New York, NY, USA, 29–39. <https://doi.org/10.1145/2984511.2984512>
- [5] Xiang 'Anthony' Chen, Ye Tao, Guanyun Wang, Runchang Kang, Tovi Grossman, Stelian Coros, and Scott E. Hudson. 2018. Forte: User-Driven Generative Design. In *Proceedings of the 2018 CHI Conference on Human Factors in Computing Systems* (Montreal QC, Canada) (*CHI '18*). Association for Computing Machinery, New York, NY, USA, Article 496, 12 pages. <https://doi.org/10.1145/3173574.3174070>
- [6] Robert M. Friedman, Kim D. Hester, Barry G. Green, and Robert H. LaMotte. 2008. Magnitude estimation of softness. *Experimental Brain Research* 191, 2 (aug 2008), 133–142. <https://doi.org/10.1007/s00221-008-1507-5>
- [7] Anhong Guo, Jeeeon Kim, Xiang 'Anthony' Chen, Tom Yeh, Scott E. Hudson, Jennifer Mankoff, and Jeffrey P. Bigham. 2017. Facade: Auto-generating Tactile Interfaces to Appliances. In *Proceedings of the 2017 CHI Conference on Human Factors in Computing Systems* (Denver, Colorado, USA) (*CHI '17*). ACM, New York, NY, USA, 5826–5838. <https://doi.org/10.1145/3025453.3025845>
- [8] Roland Harper and S. S. Stevens. 1964. Subjective Hardness of Compliant Materials. *Quarterly Journal of Experimental Psychology* 16, 3 (1964), 204–215. <https://doi.org/10.1080/17470216048416370> arXiv:<https://doi.org/10.1080/17470216048416370>
- [9] Zvi Hashin and Shmuel Shtrikman. 1963. A variational approach to the theory of the elastic behaviour of multiphase materials. *Journal of the Mechanics and Physics of Solids* 11, 2 (1963), 127–140.
- [10] Mark Hollins, Sliman Bensmaia, Kristie Karlof, and Forrest Young. 2000. Individual differences in perceptual space for tactile textures: Evidence from multidimensional scaling. *Perception & Psychophysics* 62, 8 (01 Dec 2000), 1534–1544. <https://doi.org/10.3758/BF03212154>
- [11] Alexandra Ion, Johannes Frohnhofer, Ludwig Wall, Robert Kovacs, Mirela Alistar, Jack Lindsay, Pedro Lopes, Hsiang-Ting Chen, and Patrick Baudisch. 2016. Metamaterial Mechanisms. In *Proceedings of the 29th Annual Symposium on User Interface Software and Technology* (Tokyo, Japan) (*UIST '16*). ACM, New York, NY, USA, 529–539. <https://doi.org/10.1145/2984511.2984540>
- [12] L. A. Jones and I. W. Hunter. 1990. A perceptual analysis of stiffness. *Experimental Brain Research* 79, 1 (01 Jan 1990), 150–156. <https://doi.org/10.1007/BF00228884>
- [13] Rubaiat Habib Kazi, Tovi Grossman, Hyunmin Cheong, Ali Hashemi, and George Fitzmaurice. 2017. DreamSketch: Early Stage 3D Design Explorations with Sketching and Generative Design. In *Proceedings of the 30th Annual ACM Symposium on User Interface Software and Technology* (Qubec City, QC, Canada) (*UIST '17*). ACM, New York, NY, USA, 401–414. <https://doi.org/10.1145/3126594.3126662>
- [14] Ranjitha Kumar, Jerry O. Talton, Salman Ahmad, and Scott R. Klemmer. 2011. Bricolage: Example-based Retargeting for Web Design. In *Proceedings of the SIGCHI Conference on Human Factors in Computing Systems* (Vancouver, BC, Canada) (*CHI '11*). ACM, New York, NY, USA, 2197–2206. <https://doi.org/10.1145/1978942.197926>
- [15] Johannes Kunz and Mario Studer. 2006. Determining the modulus of elasticity in compression via Shore-A hardness. *Kunststoffe international* 96, 6 (2006), 92–94.
- [16] Brian Lee, Savil Srivastava, Ranjitha Kumar, Ronen Braffman, and Scott R. Klemmer. 2010. Designing with Interactive Example Galleries. In *Proceedings of the SIGCHI Conference on Human Factors in Computing Systems* (Atlanta, Georgia, USA) (*CHI '10*). ACM, New York, NY, USA, 2257–2266. <https://doi.org/10.1145/1753326.1753667>
- [17] Raz Leib, Ilana Nisky, and Amir Karniel. 2010. Perception of Stiffness during Interaction with Delay-Like Nonlinear Force Field. In *Haptics: Generating and Perceiving Tangible Sensations*, Astrid M. L. Kappers, Jan B. F. van Erp, Wouter M. Bergmann Tiest, and Frans C. T. van der Helm (Eds.). Springer Berlin Heidelberg, Berlin, Heidelberg, 87–92.
- [18] Jonas Martinez, Jérémie Dumas, and Sylvain Lefebvre. 2016. Procedural Voronoi Foams for Additive Manufacturing. *ACM Trans. Graph.* 35, 4, Article 44 (July 2016), 12 pages. <https://doi.org/10.1145/2897824.2925922>
- [19] Jonas Martinez, Samuel Hornus, Haichuan Song, and Sylvain Lefebvre. 2018. Polyhedral Voronoi Diagrams for Additive Manufacturing. *ACM Trans. Graph.* 37, 4, Article 129 (July 2018), 15 pages. <https://doi.org/10.1145/3197517.3201343>
- [20] Jonas Martinez, Haichuan Song, Jérémie Dumas, and Sylvain Lefebvre. 2017. Orthotropic K-nearest Foams for Additive Manufacturing. *ACM Trans. Graph.* 36, 4, Article 121 (July 2017), 12 pages. <https://doi.org/10.1145/3072959.3073638>
- [21] Vittorio Megaro, Jonas Zehnder, Moritz Bächer, Stelian Coros, Markus Gross, and Bernhard Thomaszewski. 2017. A Computational Design Tool for Compliant Mechanisms. *ACM Trans. Graph.* 36, 4, Article 82 (July 2017), 12 pages. <https://doi.org/10.1145/3072959.3073636>
- [22] Jean-Claude Michel, Hervé Moulinec, and P Suquet. 1999. Effective properties of composite materials with periodic microstructure: a computational approach. *Computer methods in applied mechanics and engineering* 172, 1-4 (1999), 109–143.
- [23] Graeme W Milton. 2002. The theory of composites. *The Theory of Composites*, by Graeme W. Milton, pp. 748. ISBN 0521781256. Cambridge, UK: Cambridge University Press, May 2002. (2002), 748.
- [24] Viktor Miruchna, Robert Walter, David Lindbauer, Maren Lehmann, Regine von Klitzing, and Jörg Müller. 2015. GelTouch: Localized Tactile Feedback Through Thin, Programmable Gel. In *Proceedings of the 28th Annual ACM Symposium on User Interface Software & Technology* (Charlotte, NC, USA) (*UIST '15*). ACM, New York, NY, USA, 3–10. <https://doi.org/10.1145/2807442.2807487>
- [25] Stefanie Mueller, Sanghi Im, Serafima Gurevich, Alexander Teibrich, Lisa Pfisterer, François Guimbretière, and Patrick Baudisch. 2014. WirePrint: 3D Printed Previews for Fast Prototyping. In *Proceedings of the 27th Annual ACM Symposium on User Interface Software and Technology* (Honolulu, Hawaii, USA) (*UIST '14*). ACM, New York, NY, USA, 273–280. <https://doi.org/10.1145/2642918.2647359>
- [26] Jifei Ou, Lining Yao, Daniel Tauber, Jürgen Steimle, Ryuma Niiyama, and Hiroshi Ishii. 2013. jamSheets: Thin Interfaces with Tunable Stiffness Enabled by Layer Jamming. In *Proceedings of the 8th International Conference on Tangible, Embedded and Embodied Interaction* (Munich, Germany) (*TEI '14*). ACM, New York, NY, USA, 65–72. <https://doi.org/10.1145/2540930.2540971>
- [27] Julian Panetta, Qingnan Zhou, Luigi Malomo, Nico Pietroni, Paolo Cignoni, and Denis Zorin. 2015. Elastic Textures for Additive Fabrication. *ACM Trans. Graph.* 34, 4, Article 135 (July 2015), 12 pages. <https://doi.org/10.1145/2766937>
- [28] Michal Piovarči, David I. W. Levin, Danny M. Kaufman, and Piotr Didyk. 2018. Perception-aware Modeling and Fabrication of Digital Drawing Tools. *ACM Trans. Graph.* 37, 4, Article 123 (July 2018), 15 pages. <https://doi.org/10.1145/3197517.3201322>
- [29] Michal Piovarči, David I. W. Levin, Jason Rebello, Desai Chen, Roman Đurković, Hanspeter Pfister, Wojciech Matusik, and Piotr Didyk. 2016. An Interaction-aware, Perceptual Model for Non-linear Elastic Objects. *ACM Trans. Graph.* 35, 4, Article 55 (July 2016), 13 pages. <https://doi.org/10.1145/2897824.2925885>
- [30] Assaf Pressman, Amir Karniel, and Ferdinando A. Mussa-Ivaldi. 2011. How Soft Is That Pillow? The Perceptual Localization of the Hand and the Haptic Assessment of Contact Rigidity. *Journal of Neuroscience* 31, 17 (2011), 6595–6604. <https://doi.org/10.1523/JNEUROSCI.4656-10.2011> arXiv:<https://www.jneurosci.org/content/31/17/6595.full.pdf>
- [31] Christian Schumacher, Bernd Bickel, Jan Rys, Steve Marschner, Chiara Daraio, and Markus Gross. 2015. Microstructures to Control Elasticity in 3D Printing. *ACM Trans. Graph.* 34, 4, Article 136 (July 2015), 13 pages. <https://doi.org/10.1145/2766926>
- [32] Christian Schumacher, Steve Marschner, Markus Gross, and Bernhard Thomaszewski. 2018. Mechanical Characterization of Structured Sheet Materials. *ACM Trans. Graph.* 37, 4, Article 148 (July 2018), 15 pages. <https://doi.org/10.1145/3197517.3201278>
- [33] Ole Sigmund. 1995. Tailoring materials with prescribed elastic properties. *Mechanics of Materials* 20, 4 (1995), 351 – 368. [https://doi.org/10.1016/0167-6636\(94\)00069-7](https://doi.org/10.1016/0167-6636(94)00069-7)
- [34] Smooth-On. 2020. Durometer Shore Hardness Scale. <https://www.smooth-on.com/page/durometer-shore-hardness-scale/>. (Accessed on 08/06/2020).
- [35] Oluwaseyi (Seyi) Sosanya. 2014. 3D Weaver. <https://www.sosafresh.com/3d-weaver/>. (Accessed on 08/11/2020).
- [36] Mandayam A Srinivasan and Robert H LaMotte. 1995. Tactual discrimination of softness. *Journal of Neurophysiology* 73, 1 (1995), 88–101.
- [37] Wouter M. Bergmann Tiest and Astrid M.L. Kappers. 2006. Analysis of haptic perception of materials by multidimensional scaling and physical measurements of roughness and compressibility. *Acta Psychologica* 121, 1 (Jan. 2006), 1–20. <https://doi.org/10.1016/j.actpsy.2005.04.005>
- [38] W. M. Bergmann Tiest and A. M. L. Kappers. 2009. Cues for Haptic Perception of Compliance. *IEEE Transactions on Haptics* 2, 4 (Oct 2009), 189–199. <https://doi.org/10.1109/TOH.2009.16>
- [39] Cesar Torres, Tim Campbell, Neil Kumar, and Eric Paulos. 2015. HapticPrint: Designing Feel Aesthetics for Digital Fabrication. In *Proceedings of the 28th Annual ACM Symposium on User Interface Software & Technology* (Charlotte, NC, USA) (*UIST '15*). ACM, New York, NY, USA, 583–591. <https://doi.org/10.1145/2807442.2807492>
- [40] Ultimaker. 2020. Ultimaker Cura infill settings. <https://ultimaker.com/en/resources/52670-infill>.
- [41] Ultimaker 2020, Apr (Last commit). CuraEngine. <https://github.com/Ultimaker/CuraEngine>.
- [42] Mian Wei and Karan Singh. 2017. Bend-a-rule: A Fabrication-based Workflow for 3D Planar Contour Acquisition. In *Proceedings of the 1st Annual ACM Symposium on Computational Fabrication* (Cambridge, Massachusetts) (*SCF '17*). ACM, New York, NY, USA, Article 5, 7 pages. <https://doi.org/10.1145/3083157.3083164>

A APPENDIX

Slicing parameters and their effects in resulting softness based on the experiment settings. Other than listed in Table 3, parameters (e.g. support type, enable retraction, etc.) showed no significant effect on softness.

Slicing Experiment		Results, Findings, & Rationale
Param	settings	
Layer height	0.1 – 0.3mm by 0.05mm increments	Increasing it over 0.25mm loosens layer binding strength, with minimal effect on softness.
Shell thickness	0.2 – 1.2mm by 0.2mm increments	No effects on softness appearing on the top contact surface, only to vertical walls.
Flow rate	80 - 120 % by 5 % increments	More material extruded by higher flow rate resulting in a stiffer object, but the value cannot be below 100 % to guarantee printability.
Printing speed	5 – 30mm/s, by 5mm/s increments	The faster speed is, the harder outcome object is*. Speed cannot be faster than 20mm/s to ensure printability in flexible material printing.
Number of top layers	1 - 5, by increments of 1	Layer count is determined by the top/bottom layer thickness divided by layer height (rounded up to the nearest integer by CURA), so not freely controllable.
Infill type	Selection of patterns	Limited in available types, confounding factors on softness, making it hard for granular control.
Infill density	5 % - 100 %, by 10 % increments**	The widest range of softness with fine granularity of softness achieved, and guaranteed printability.
Print temp.	from 200 - 240, by 5 degrees increments	The higher, the softer, partly due to porosity formed by hydrogen absorbed from the air by material.

Table 3: Experiments between slicing parameter as variables to measure its impact in produced softness. *Empirical finding, clear causality effect has yet to be proven. **We expanded the test with custom created wall spacing, by calculating % of empty spaces that does not support the top cover in a given flat region

B APPENDIX

Here we introduce how we model the softness by controlling the wall spacing as factor, then validate our model. We can compute the number of interior walls in a given square mesh as follows:

$$N_w = W_o / (L_d + T_s) \quad (2)$$

Where N_w (integer) denotes the computed number of internal walls to support the top, W_o refers to the width of the object, L_d refers to the spacing between two adjacent walls, and T_s refers to the thickness of each wall, currently set as default to the nozzle diameter.

To define a trend line to predict targeting softness by a printing parameter, we conducted a standard data fitting. The key parameter of producing different softness in our mechanism is infill density, in turn, represented as wall spacing in linear infill. The relationship between wall spacing and softness is shown in Figure 17, and we fit 3 different mathematical models to the data.

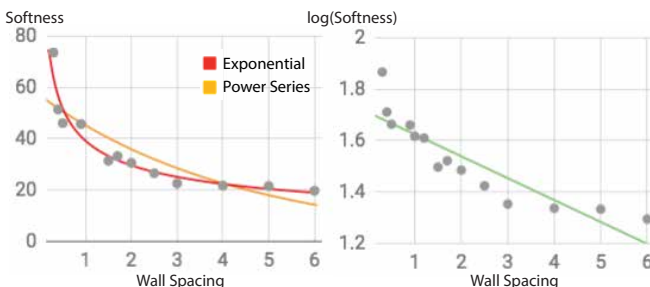


Figure 17: Finding trend lines using an exponential model, power series, and linear model (by taking logs on exponential model) ($R^2 = 0.728, 0.926, 0.792$)

Here we get three equations that explain the data correlations better, with higher R^2 than others. For example, the equation derived by the power series fit is as follows:

$$S = \alpha \times L_d^{-\beta} \quad (3)$$

Where L_d denotes our variables (ranging from 0.3mm to 6mm), spacing between walls, and S denotes produced softness by given variable values. For Soft PLA, $\alpha = 38.2$ and $\beta = 0.408$, while for TPU, $\alpha = 43.9$, $\beta = 0.415$.

Our goal is to enable the system to compute an exact spacing given a user specified softness level. When a user enters their desired softness level (S), the system needs to calculate the line distance (L_d) to leave gaps between vertical walls. This gives us the following by inverse of the Eq.(3):

$$L_d = e^{-\frac{1}{\beta} \times (\ln S - \ln \alpha)} \quad (4)$$

Where L_d denotes computed line distance, and S refers to the input, a desired softness level. For example, to fabricate an object with softness 35 using Soft PLA, infill wall spacing is calculated by $e^{-\frac{1}{0.408} \times (\ln 35 - \ln 38.2)}$, which is 1.2391mm. Then this gap is used to build a number of walls inside of the object by equation (2) in the system.

B.1 Validation

To prevent over/underfitting and validate our models, we printed additional samples with wall separation distances computed from a set of input softness values using all three fitted models. Table 4 summarizes the input target softness, the computed wall separation and the corresponding actual softness measured by a Durometer.

Softness Input	Linear $L_d \Rightarrow S_p$	Exponential $L_d \Rightarrow S_p$	Power Series $L_d \Rightarrow S_p$
15	6.74 \Rightarrow 18.83	6.19 \Rightarrow 18.83	9.88 \Rightarrow 15.66
25	3.77 \Rightarrow 20.33	3.64 \Rightarrow 22.33	2.82 \Rightarrow 25.5
35	1.81 \Rightarrow 35.83	1.96 \Rightarrow 34	1.23 \Rightarrow 35.83
40	1.04 \Rightarrow 42.5	1.29 \Rightarrow 43	0.89 \Rightarrow 41.16
45	0.35 \Rightarrow 61.6	0.70 \Rightarrow 47.83	0.66 \Rightarrow 47.83

Table 4: Softness reproduction validation by random sampling of target softness. Power series fit generates the least errors. (errors STD=7.87, 2.86, 0.94)

Based on these validations, we conclude that the power series model best suits to reproduce specified softness without over/underfitting.

B.2 Radial walls

For non-cuboid objects such as bike handles, where user's force is applied around a curved surface, internal support structures should be distributed evenly below this surface. For perfect cylinders, internal structures that support such surface is achieved by a radial distribution of walls. Similar to the cuboid case, the density of such radial infill walls will significantly influence the print's softness. Instead of changing the line spacing (L_d from eq. 3), we change the arc spacing, L_{arc} , to achieve different infill density, where arc spacing can be controlled via the angle, θ , between two adjacent infill walls (i.e. $L_{arc} = 2\pi r \times \frac{\theta}{360^\circ}$ where r is the radius of the cylinder). With arc spacing replacing line spacing, we can reapply our data fitting model (eq. (3)-(4)) to find α , β , where $\alpha = 152$, and $\beta = 0.852$ for Soft PLA, and $\alpha = 151$, and $\beta = 0.792$ for TPU.